Improvement Structural and Optical Properties of ZnO/ PVA Nanocomposites

A.F. Mansour, S.F. Mansour and M. A. Abdo
Physics Department, Faculty of Science, Zagazig University, Egypt

Abstract: *The structural and optical properties of polyvinyl alcohol (PVA) doped with different concentrations (0, 0.15, 0.5, 1, 2, 2.5, and 3 wt %) of ZnO nanoparticles were studied. ZnO nanoparticles were prepared by the sol- gel methode, and nanocomposite films were prepared using the solution casting methode. Nanocomposites films were characterized by X-ray diffraction (XRD), Fourier Transformer Infrared (FTIR). The optical properties and optical constants of ZnO/ PVA nanocomposite films have been investigated by means of transmittance and reflectance spectra. The optical band gap E_g was determined and the optical absorption spectra showed that the absorption mechanism is a direct transition. The refractive index (n), extinction coefficient (k) and dielectric constant of the films were determined. We have applying Wemple – Didomenico single oscillator model to calculate the dispersion of the refractive index.. The nanocomposite ZnO/ PVA (3% wt) shows the lower optical band gap value and the higher optical conductivity as compared to other concentration of ZnO.*

Keywords: *Polyvinyl Alcohol (PVA); Zinc Oxide ZnO; nanocomposite; XRD; FTIR; optical properties.*

I. Introduction

Polymer- based metal oxide nanocomposites have many applications because of their electron transport, mechanical and optical properties in medical and engineering technology [1, 2].

Polyvinyl alcohol (PVA) is a polymer with several interesting physical properties, which are very useful in technical application. PVA is a semi crystalline, water soluble , low electrical conductivity material, and has excellent film forming and adhesive properties making it have many technological, pharmaceutical and biomedical applications [3,4].

Zinc oxide (ZnO) based polymeric nanocomposite materials are very interesting because of their good transparency, high electron mobility [5, 6], direct wide band gap (3.37 eV at room temperature) [7]. This enables applications in optoelectronics in the blue/UV region, including light-emitting diodes, laser diodes and photo detectors [8- 10], short-wavelength light emitting diodes, transparent conductors, dye-sensitized solar cells, piezoelectric materials, gas sensors, photovoltaic cells, varistors (also called as variable resistors), as a high resistance semiconducting device and fully transparent thin film transistors [11].

In the present work ZnO nanoparticles have been synthesized by sol–gel method. ZnO/ PVA nanocomposite films with different concentrations of nano ZnO were prepared using easy and low cost solution casting method. The samples were characterized by XRD, FTIR, and UV– visible spectroscopy. Also, we had studied the optical properties of ZnO/ PVA nanocomposites based on ZnO nanoparticles as inorganic filler material and PVA as the main matrix.

II. Experimental

2.1. Materials

Polyvinyl alcohol (PVA) from Sigma Aldrich, with average molecular weight of 50.000 – 85.000 and 97% hydrolyzed was used without further purification. Zinc nitrate $[Zn(NO_3)_2.6H_2O]$ and ethylene glycol $(C_2H_6O_2)$ also were purchased from Aldrich. Reactant solutions were made in doubly distilled water.

2.2. Synthesis of ZnO nanoparticles

Nano-sized particles of ZnO were prepared using sol gel method [12, 13]. The proper amounts of zinc nitrate hexahydrate $(Zn(NO_3)_2 \cdot 6H_2O)$ was dissolved in distilled water under constant stirring and heated to about 90^oC for 1 h. The solution was added to ethylene glycol $(C_2H_6O_2)$ maintaining the molar ratio between the metal nitrates and the ethylene glycol as 1:1. This mixed solution was then stirred for 2h to achieve good homogeneity. The precursor mixture was heated to allow evaporation then combustion to obtain finally the desired product zinc oxide (ZnO) in the form of ash powder.

2.3. Preparation of ZnO/ PVA nanocomposite films

The nanocomposite films were prepared by the well known solution casting technique. In this method 7g of (PVA) powder was dissolved in 80 ml of de-ionized water by stirring and heated kindly using a

magnetic stirrer with hot plate, for complete dissolution without thermal decomposition of the polymer, until the polymer was completely dissolved and a clear viscous solution is formed. The prepared ZnO nanopowder was added into the aqueous solution of PVA in the following composition (w/w between ZnO and PVA solution concentration): 0%, 0.15%, 0.5%, 1%, 2%, 2.5%, and 3% then stirred carefully by using magnetic stirrer until well dispersion ZnO/ PVA was obtained. Each mixture is put in a Petri dish and leave to dry in a dust free chamber at room temperature to obtain the nanocomposite films.

2. 4. Characterization
        The X-ray diffraction (XRD) patterns of the pure PVA film, nano ZnO powder and the polymer nanocomposite films were recorded at room temperature using an X-ray powder diffractometer (Shimadzu XRD 6000) equipped with Cu K_α as radiation source (λ = 1.54Å.) in the 2θ (Bragg angles) range($10^o \leq 2\theta \leq 80^o$) to report the information about their structure. The Fourier transform infrared (FTIR) spectra of the nano powder and the nanocomposites were analyzed in the range 400– 4000 cm^{-1} using Jasco instrument (Model 6100, Japan) in the absorbance mode at a resolution of 4.0 cm^{-1}. The absorbance spectra (A) and the transmittance spectra (T) of the films were recorded at 200–1100 nm wavelength using a dual beam (UVS-2800) UV–Visible spectrophotometer.

III.   Results And Discussion
3.1. X-Ray diffraction analysis
        The X-ray diffraction pattern (XRD) for pure polyvinyl alcohol (PVA) sample is shown in figure (1a). The XRD pattern showed a strong broad diffraction peak located at 2θ= 20.12^o which corresponding to (101) reflection plane of PVA and a more peak at 41.62^o indicating the semi-crystalline nature of PVA i.e., presence of crystalline and amorphous regions [14, 15]. This diffraction peak confirmed that, obtained polyvinyl alcohol (PVA) is pure polyvinyl alcohol (PVA) without any other impurities.
        The XRD pattern for pure Zinc oxide (ZnO) sample is shown in figure (1b). These observable peaks, at scattering angles 2θ= 31.68^o, 34.34.4^o, 36.16^o, 47.52^o, 56.48^o, 62.88^o, 66.24^o, 67.84^o, 68.96^o, 72.48^o and 76.8^o are correspond to reflections from: 100, 002, 101, 102, 110, 103, 200, 112, 201, 004 and 202 crystal planes, confirmed the formation of the as prepared ZnO in a pure single hexagonal phase. The XRD pattern was indexed and compared with JCPDS card no. 36-1451 which correspond to the hexagonal wurtzite structure of ZnO. The expanded peaks in XRD pattern indicate ultra-fine nature of the crystallites. It is clear; the peaks are very sharp, indicating the complete formation of crystal structure.
        The X-ray diffraction patterns for ZnO/ PVA nanocomposite films as shown in figure (1c). XRD patterns of all ZnO/ PVA nanocomposite films showed a broad peak at 2θ ≈ 19.90^o, which is attributed to the polyvinyl alcohol (PVA). Also, a small diffraction peaks observed at 2θ ≈ 31.96^o, 34.67^o, 36.44^o, 48°, 56.86^o, 63.12^o, and 68.2^o which is attributed to the reflection from: 100, 002, 101, 102, 110, 103, and 112 confirmed the presence of the zinc oxide (ZnO) nano particles. The diffraction peaks which attributed to ZnO is very small compared with that of PVA, because the concentration of ZnO is very low compared with that of PVA. This small peak increases by increasing ZnO content reaching 3%, as shown in figure (1c). The results indicate that the nanocomposite films consists only of two phases namely PVA and ZnO and no other phases was detected which assure its successful preparation. The lattice parameters "a" and "c" of the polycrystalline ZnO and ZnO in ZnO/ PVA nanocomposites films are calculated respectively with (100) and (002) orientations using the relation [16]:

$$\frac{1}{d^2} = \frac{4}{3}(\frac{h^2 + hk + k^2}{a^2}) + \frac{l^2}{c} \qquad (1)$$

        The obtained lattice parameters values for pure ZnO powders are a= 0.325 nm and c= 0.521 nm are in a very good agreement with those reported in JCPDS card no. 36-1451. By increasing ZnO content in ZnO/ PVA nanocomposites, there were slight change in the position of the peaks indicating a corresponding change in lattice constants of the two phases but the obtained lattice parameters nearly have the same values (a= 0.322 nm ± 0.001) and (c= 0.516 nm ± 0.001). This indicates that ZnO nanoparticles have retained its structure even though it is capped PVA after formation of nanocomposite films, i.e., there is no interaction between polyvinyl alcohol and zinc oxide in forming nanocomposites. The crystal size of ZnO in pure nanopowder and nanocomposite films is calculated using the, Debye-Scherrer formula [17]:

$$D = \frac{0.9\lambda}{\beta \cos\theta} \qquad (2)$$

D is the grain size, λ is the wavelength of the X-ray radiation used, β is the full width at half maximum (FWHM) of the diffraction peak and θ is the Bragg diffraction angle of the XRD peak. The average crystallite size estimated is ≈ 41nm.

3.3. Fourier Transformer Infrared (FTIR) Spectroscopic Analysis:
Fourier transformer infrared spectroscopy (FTIR) is one of the most powerful techniques to investigate a multi-component system, such as polymer composite, because it provides information for both compositions.

The FTIR spectra for pure PVA, ZnO/ PVA nanocomposite films and ZnO are shown in figure (2). In the spectra of pure PVA and ZnO/ PVA nanocomposites, the broad and strong band centered at 3340 cm^{-1} is assigned to the stretching vibration of hydroxyl group (OH) [18]. The strong band at 2940 cm^{-1} is assigned to the band of asymmetric CH$_2$ stretching [19]. The two bands observed at 1712 and 1658 cm^{-1} are assigned to the stretching vibrational band of C=O [20]. The two bands observed at 1427 and 1330 cm^{-1} are assigned as CH$_3$ bending vibration and CH$_2$ stretching respectively [21]. The band at 1090 cm^{-1} arises from the C–O stretching vibration while the band at 920 cm^{-1} results from CH$_2$ rocking vibration [22]. Also, the band at 850 cm^{-1} result from C–C stretching vibration and that at 660 cm^{-1} arises from out of plane OH bending [14]. The band at 432cm^{-1} is assigned to the stretching vibration of Zn-O bond [23]. FTIR spectra of PVA, ZnO and ZnO/ PVA nanocomposites indicating that there are no interactions between polyvinyl alcohol and zinc oxide in forming nanocomposites.

3.4. Optical properties:
The UV–visible absorption spectroscopy is a usual technique to examine the optical properties of nano sized particles and hence nanocomposite films.

Figure (3) shows UV-visible absorption spectra of pure PVA and ZnO/ PVA nanocomposite films. The absorption spectrum of pure PVA has one broad absorbance band at 290 nm and one weak band or shoulder at 330 nm. These bands are assigned to the electronic transitions $\pi \rightarrow \pi^*$ and $n \rightarrow \pi^*$, respectively [24, 25]. The absorbance spectra of the ZnO/ PVA nanocomposite films are containing the fundamental peak of the PVA and further absorbance band at 375 nm, corresponding to ZnO [14]; which be 5nm bleu shift in comparison comparing with the ZnO bulk material (380 nm) at room temperature [19, 26]. This blue shift is due to the quantum confinement effect i.e., due to the reduction in the crystallite size [27, 28]. The absorbance of the nanocomposite films increase with increasing ZnO concentration. This is because of the added ZnO nanoparticles absorb the incident radiation by its free electrons. There is no shift in the absorption edge of PVA and ZnO; indicating no clear interaction between PVA matrix and ZnO nanoparticles.

3.4.1. Determination of optical band gap:
The optical transitions in nanocomposite films can be easily understood by determining the optical band gap by Tauc's plot [29, 30]. The frequency dependent absorption coefficient is given by

$$\alpha h \nu = B(h \nu - E_{op})^n \qquad (3)$$

α is the absorption coefficient, which calculated using the Beer- Lambert's relation [31] $\alpha = 2.303 \dfrac{A}{t}$; A and t are the absorbance and the thickness of the film. B is the parameter that depends on the inter band transition probability, hν is the incident photon energy, E$_g$ is the optical band gap and (n) is an index characterizing the nature of the electronic transitions causing the optical absorption. n can take values 1/2, 3/2, 2, and 3 for direct allowed, direct forbidden, indirect allowed and indirect forbidden transitions, respectively. Figure (4a) show the relation between absorption edge $(\alpha h \nu)^2$ for pure PVA and ZnO/ PVA nanocomposites as a function of photon energy (hν). At extension of the curve to the value $(\alpha h \nu)^2 = 0$, we get the direct band gap of the nanocomposites. The obtained values of optical band gap of the nanocomposites are tabulated in table (1). It is showed that the values of energy gap decrease with increasing ZnO concentration, as shown in figure (4b). This decrease due to creation of new levels in the band gap, lead to facilitate the crossing of electrons from the valence band to these local levels to the conduction band, consequently the conductivity increase and the band gap decreases [32, 33].

3.4.2. Determination of optical constants:
The refractive index (n) plays a very important role in optical communication and designing of the optical devices. One of the methods for calculating the refractive index (n) is by using the reflectance (R) and the extinction coefficient (k), where k= $\alpha \lambda / 4\pi$, of films [34]:

$$n = \frac{(1+R)}{(1-R)} + \sqrt{\frac{4R}{(R-1)^2} - k^2} \qquad (4)$$

Figure (5) shows the refractive index (n) of pure PVA and ZnO/ PVA nanocomposite films as a function of wavelength. The refractive index increases with increasing ZnO concentration; due to the density of the nanocomposite films is increased with doping. In fact, when the incident light interacts with a material has a large amount of particles, the refraction will be high and hence the refractivity of the films will be increased.

In the normal dispersion region (the transparent region), the refractive index dispersion has been analyzed using the single oscillator model developed by Wemple and DiDomenico [35, 36].

$$n^2 - 1 = \frac{E_o E_d}{E_o^2 - (h\nu)^2} \tag{5}$$

Where, E_o is the oscillator energy (which is a measure of the average excitation energy for electronic transitions), and E_d is the dispersion energy (which is a measure of the average strength of inter-band optical transitions).

The values of E_o and E_d can be obtained from the intercept and slope of the linear fitted lines by plotting $1/(n^2- 1)$ versus $(h\nu)^2$ as shown in figure (6). The obtained values of E_o and E_d are tabulated in table (1). It can be discerned from table (1) that the values of E_o, decrease with increasing concentration of ZnO nanoparticles in PVA matrix. This decrease because of increasing the localized states in the energy gap which in turn enhances the low energy transitions leading to a decrease in the value of E_o. The dispersion energy E_d, is associated with changes in the structural order of the material [37], which explain the increase in E_d values with increasing ZnO concentration. The oscillator energy E_o is related empirically to the optical band gap E_g; for our ZnO/ PVA nanocomposites $E_o=1.32E_g$. The static refractive index n_o, at zero photon energy and then the static dielectric constant $\varepsilon_s= n_o^2$, are also evaluated and tabulated in table (1). The static refractive index and the static dielectric constant of ZnO/ PVA nanocomposites increase with increasing ZnO concentration.

To calculate the average inter band oscillator wavelength λ_o and the average oscillator strength S_o, for ZnO/ PVA nanocomposite films, the single oscillator model equation has been considered as [38]:

$$\frac{n_o^2 - 1}{n^2 - 1} = 1 - (\frac{\lambda_o}{\lambda})^2 \tag{6}$$

Equation (6) can also take the form

$$n^2 - 1 = \frac{(S_o \lambda_o^2)}{1 - (\frac{\lambda_o}{\lambda})^2} \tag{7}$$

Where the average oscillator strength S_o, is defined as

$$S_o = (n_o^2 - 1) / \lambda_o^2 \tag{8}$$

Figure (7) shows the variation between $(n^2- 1)^{-1}$ and λ^{-2} at different concentration of ZnO in PVA matrix. λ_o and S_o values were obtained from the slope and intercept of $(n^2- 1)^{-1}$ versus λ^{-2} curves. From table (2) it is noticed that S_o and λ_o are increase with increasing ZnO concentration.

The obtained data of refractive index n can be further analyzed to obtain the high frequency dielectric constant ε_∞ according to the following procedure. According to Pankove [39, 40] the real part of the dielectric constant is given by:

$$\varepsilon' = n^2 - k^2 = \varepsilon_\infty - (\frac{e^2}{\pi \varepsilon_o c^2})(\frac{N}{m^*})\lambda^2 \tag{9}$$

Where ε_∞ is the high-frequency dielectric constant λ is the wavelength, e is the charge of the electron, N is the free charge-carrier concentration, ε_o is the permittivity of the free space, m^* the effective mass of the charge carriers in units of kg, and c is the velocity of light. By plotting the relation between ε' and λ^2, as shown in figure (8) we can calculate ε_∞ and (N/m^*) from the intercept and the slope of the linear portion of that curve.

Also, the long wavelength refractive index n_∞, is calculated using the relation $\varepsilon_\infty = n_\infty^2$. It is noticed that free carriers increase (N/m^*) of the ZnO/ PVA nanocomposites increase with increasing ZnO nanoparticles as shown in table (2). Furthermore, ε_∞ and n_∞ are increased with increasing ZnO content.

According to these results the optical constants of these films could be controlled by ZnO content. The quantitative measurements of these parameters may help in tailoring and modeling the properties of such films for their use in optical and optoelectronic components and devices.

The optical conductivity σ_{op} is related to refractive index (n), light speed (c) and absorption coefficient (α) by the following equation [41]:

$$\sigma_{op} = \frac{nc\alpha}{4\pi} \qquad (8)$$

The term "optical conductivity" means the electrical conductivity results from the movement of the charge carriers due to alternating electric field of the incident electromagnetic waves. Figure (9) show the optical conductivity of pure PVA and ZnO/ PVA nanocomposite films. It is noticed that the optical conductivity increases with increasing ZnO nanoparticles. This increase due to creation of new levels in the band gap, lead to facilitate the crossing of electrons from the valence band to these local levels to the conduction band, consequently the band gap decreases and the conductivity increase.

IV.   Conclusion
Nano-sized particles of ZnO were prepared using sol gel method. The nanocomposite films were prepared by the well known solution casting technique. The average crystallite size estimated from XRD is ≈ 41nm. ZnO nanoparticles enhanced the optical properties of the virgin PVA matrix. The nanocomposite with concentration (3% wt) is the characteristic one, where have the highest absorption, lowest energy gap and the highest optical conductivity. These entire advantage make the ZnO/ PVA nanocomposite with ZnO concentration (3% wt) have wide range for solar cell applications, especially for solar cells electrode instead of indium tin oxide (ITO).

References
[1].   N. Bouropoulos, G.C. Psarras, N. Moustakas, A. Chrissanthopoulos, S. Baskoutas, Phys Status Solidi A 205 (2008) 2033–2037.
[2].   J. Lee, D. Bhattacharyya, A.J. Easteal, J.B. Metson, Curr Appl Phys 8 (2008) 42–47.
[3].   C. M. Hassan, N.A. Peppas, Adv. Polym. Sci. 153 (2000) 37- 65.
[4].   M. Kokabi, M. Sirousazar, Z. Hassan, Eur. Polym. J. 43 (2007) 773- 781.
[5].   Y.W. Heo, D.P. Norton, L.C. Tien, Y. Kwon, B.S. Kang, F. Ren, Mater Sci Eng R 47 (2004)1–2.
[6].   E.M.C. Fortunato, P.M.C. Barquinha, A.C.M.B.G. Pi-mentel, A.M.F. Goncalves, A.J.S. Marques, L.M.N. Pereira. Adv Mater 17 (2005) 590–4.
[7].   A. Mang, K. Reimann and Rubenacke St, Solid State Commun, 94(1995) 251- 254.
[8].   Ü. Özgür, Ya. I. Alivov, C. Liu, A. Teke, M. A. Reshchikov, S. Dogan, V. Avrutin, S-J. Cho and H. Morkoç, J. Appl. Phys., 98 (2005) 041301.
[9].   N. H. Nickel and E. Terukov, Zinc Oxide - A Material for Micro- and Optoelectronic Applications, (ed) 2005, (Netherlands: Springer).
[10].   C. Jagadish and S. J. Pearton, Zinc Oxide Bulk, Thin Films, and Nanostructures, (ed) 2006, (New York: Elsevier).
[11].   Husam S. Al-Salman, M.J. Abdullah, Superlattices and Microstructures 60 (2013) 349–357.
[12].   Agnieszka Kołodziejczak-Radzimska and Teofil Jesionowski, Materials 7 (2014) 2833-2881.
[13].   Mamady Nassou Conde, Khalid Dakhsi, Hafid Zouihri, Karima Abdelouahdi, Larbi Laanab, Mohammed Benaissa1 and Boujemaâ Jaber, Journal of Materials Science and Engineering A 1 (2011) 985-990.
[14].   K.S. Hemalatha, K. Rukmani, N. Suriyamurthy, B.M. Nagabhushana, Materials Research Bulletin 51 (2014) 438–446.
[15].   Pal Kunal, Banthia Ajit K., and Majumdar Dipak K., AAPS Pharm SciTech 8 (1) (2007), Article 21.
[16].   y. Waseda, K. Shinoda, E. Matsubara, X-Ray Diffraction Crystallography: Introduction, Examples and Solved Problems, (Springer, New York, 2011).
[17].   B.D. Cullity, Elements of X-ray Diffraction, Reading, MA, 1978.
[18].   X Yuan., Polym. Bull. 67 (2011) 1785–1797.
[19].   Aashis S. Roy, Satyajit Gupta, S. Sidhu, Ameena Parveen, Praveen C. Ramamurthy, Composites: part B 47 (2013) 314-319.
[20].   S Gunassekaran, E Sailatha, S Sesshadri, S Kumaresan, Indian Journal of Pure and Applied Physics, 47 (2009) 12- 18.
[21].   Selda Keskin, Uslu Ibrahim, Tuncay Tunc, Mustafa Öztür, Arda Aytimur, Mater. Manuf. Processes 26 (2011) 1346- 1351.
[22].   Z. Ali, H. Youssef, T. Afify, Polym. Comp., 105 (2007) 2976- 2980.
[23].   Gutul Tatyana, Rusu Emil, Condur Nadejda, Ursaki Veaceslav, Goncearenco Evgenii and Vlazan Paulina, Beilstein J. Nanotechnol 5 (2014) 402– 406.
[24].   A. M. Shehap, Egypt. J. Splids, 1 (2008), 75-91.
[25].   Dagmara M. Sabara, Julia S. Dunne, Augusto Q.H. Pedro, Jasenka Trifunović, Balogun I.O. Idiatu, Olja Kotlicic, Adriana Serrano, Kertész István, Biotechnol Food Sci. (1) (2011) 39-49.
[26].   P. Virendra, D. Charlene, Y. Deepti, A. J. Shaikh, V. Wadanathangam, Spectrochim. Acta, Part A 65 (2006) 173- 178.
[27].   K.S. Ramaiah, A.K. Bhatanagar, R. D. Pilkington, A. E. Hillard, R. D. Tomlinson, Mater J, Sci. Mater. Elect. 11(2000) 269- 277.
[28].   Shashi B Rana, Amarpal Singh, Satbir Singh, Int. J. Nanoelectronics and Materials 6 (2013) 45- 57.
[29].   J. Tauc, A. Menth, and D. Wood, Phys .Rev. Lett. 25 (1970) 749- 752.
[30].   L. Dai, J. Li, E. Yamada, J. Appl. Polym. Sci. 86 (2002) 2342- 2347.
[31].   P.P.R. Sahay, K. Nath, S. Tewari, Cryst. Res. Technol. 42 (2007) 275- 280.
[32].   E.M. Abdul Razek, A.M. Abdugany, A.H. Oraby, G.M. Asnag, J. Eng. Technol., IJET-IJENS 12 (2012) 98- 102.
[33].   Sreetama Dutta, Bichitra N. Ganguly, J. Nanobiotechnol. 29 (2012) 10- 29.
[34].   I.S. Yahia, A. A. M. Farag, M. Cavas, F. Yakuphanoglu, Superlattice. Microst. 53 (2013) 63–75.
[35].   S. H. Wemple and M., Jr. Didomenico, Phys. Rev. B 3, (1971) 1338.

[36]. A. M. El Sayed, Ali Ibrahim, Materials Science in Semiconductor Processing 26 (2014) 320– 328.
[37]. Hussain S. Shaaker, Waleed A. Hussain and Hussain A. Badran, Advances in Applied Science Research, 5 (2012) 2940-2946.
[38]. Saini Isha, Rozra Jyoti, Chandak Navneet, Aggarwal Sanjeev, Sharma Pawan K., Sharma Annu, Materials Chemistry and Physics 139 (2013) 802-810.
[39]. J.I. Pankove, Optical Processes in Semiconductors, Prentice-Hall, New Jersey (1971).
[40]. M.S. Al-Assiri, M.M. El-Desoky, A. Alyamani, A. Al-Hajry, A. Al-Mogeeth, A.A. Bahgat, Optics & Laser Technology 42 (2010) 994–1003.
[41]. Faisal A. Mustafa, Phys. Sci. Res. Int., 1 (2013) 1-9.
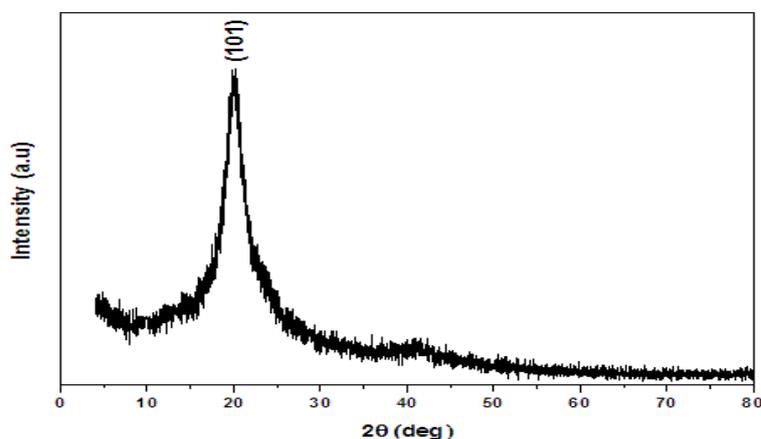
Fig. (1a): XRD pattern of pure PVA.
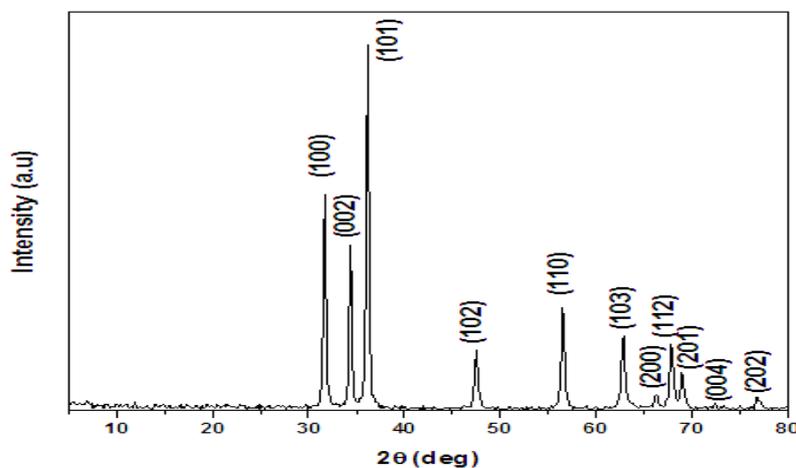
Fig. (1b): XRD pattern of pure ZnO.
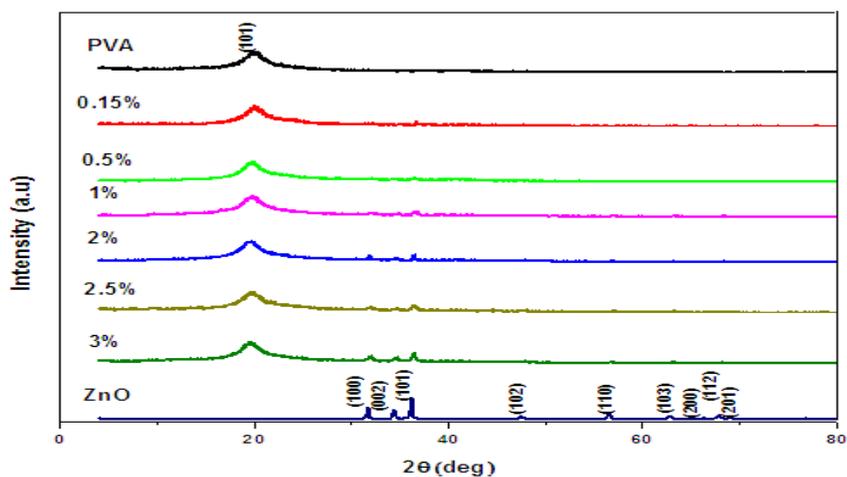
Fig. (1c): XRD pattern of PVA ZnO/ PVA films, and ZnO respectively.
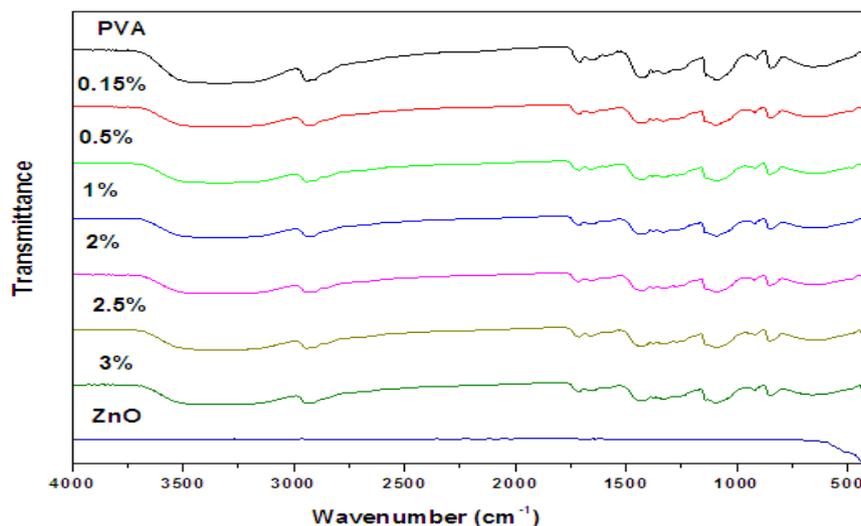
Fig. (2): FTIR spectra of: PVA, ZnO/ PVA films, and ZnO respectively.
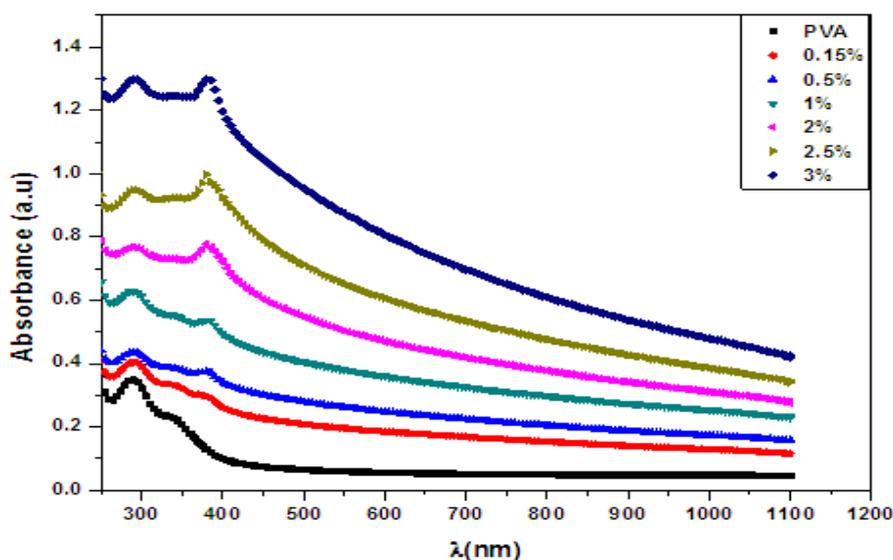
Fig. (3): UV-visible absorption spectra of pure PVA and ZnO/ PVA nanocomposite films.
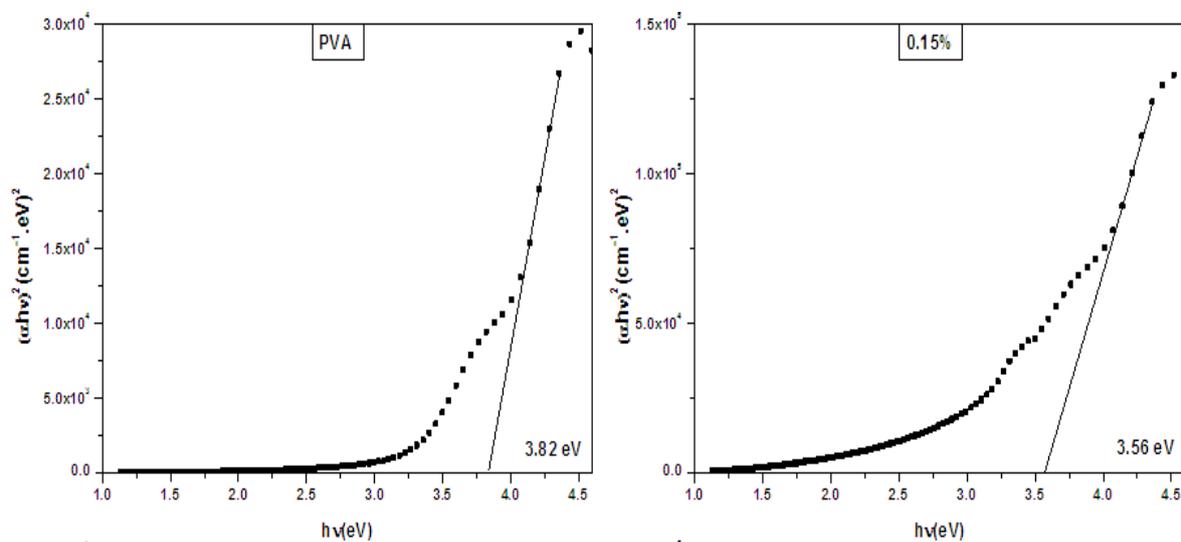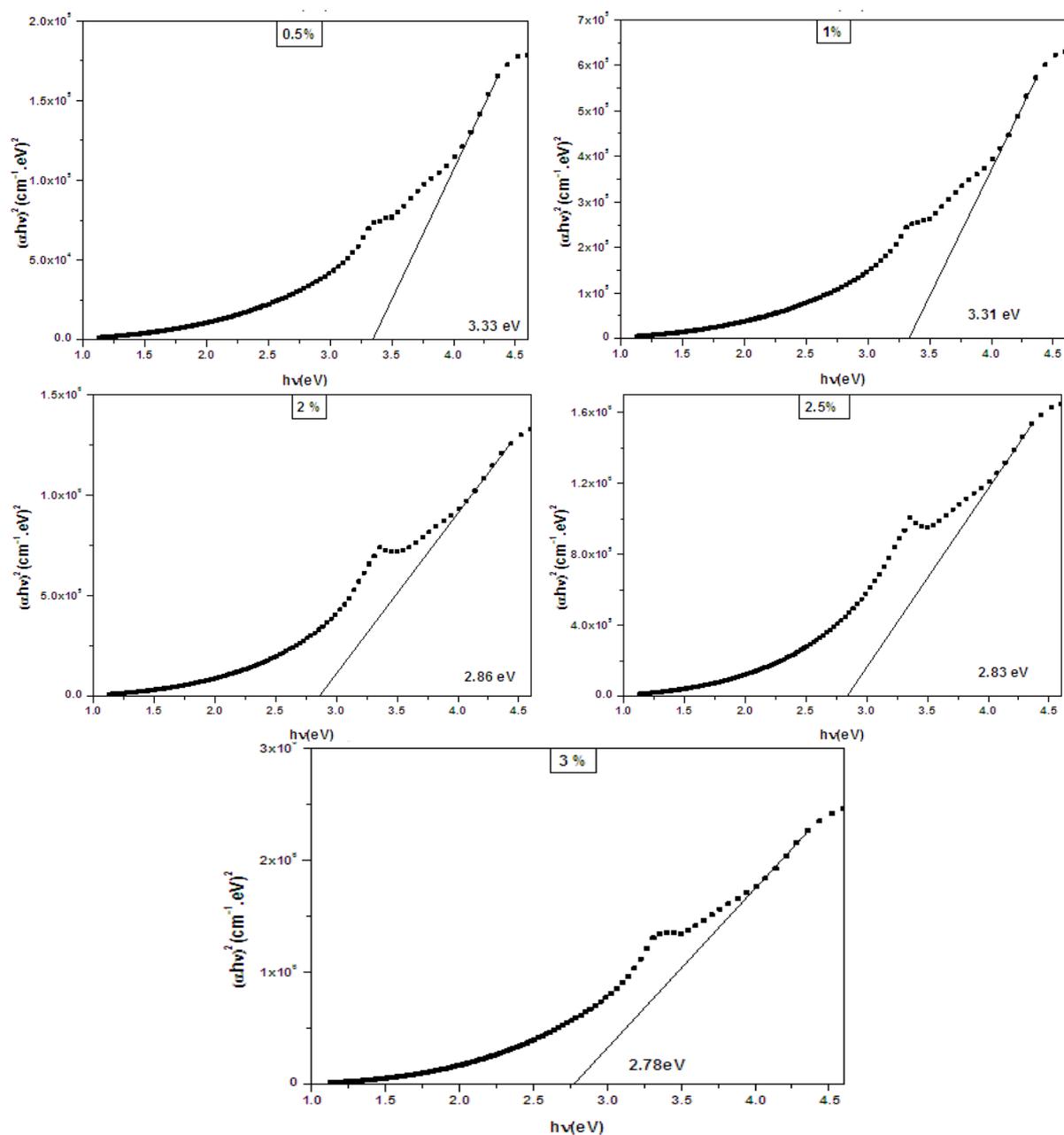
Fig. (4a): Relation between $(\alpha h\nu)^2$ and $(h\nu)$ for the pure PVA and ZnO/ PVA nanocomposite films.
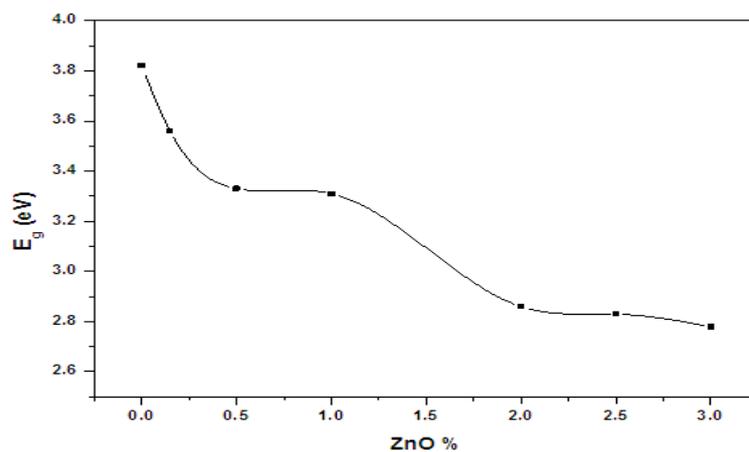
Fig. (4b): The obtained values for optical band gap as a function of ZnO concentration.
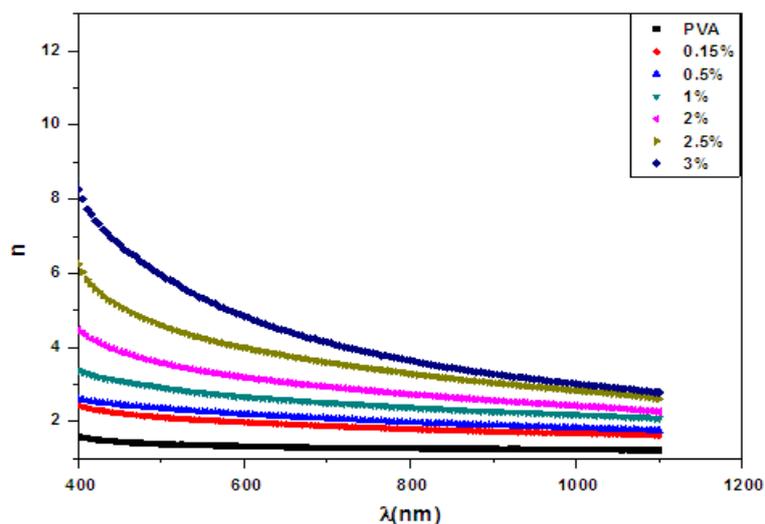
Fig. (5): The refractive index of pure PVA and ZnO/ PVA nanocomposite films.
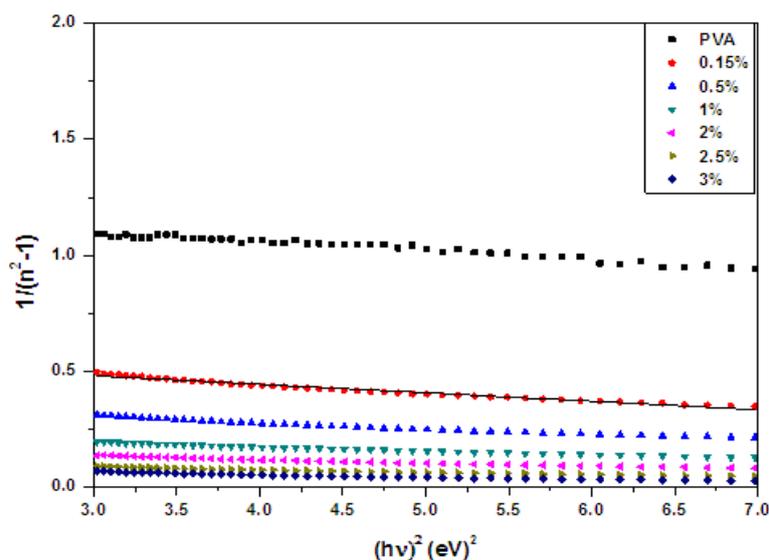
Fig. (6): Relation between $1/(n^2 - 1)$ and $(h\nu)^2$ for pure PVA and ZnO/ PVA nanocomposites.
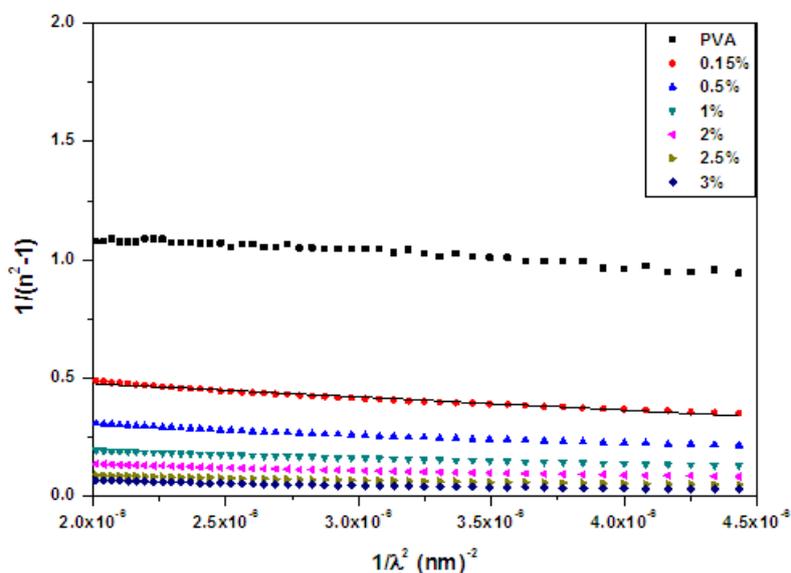
Fig. (7): Relation between $1/(n^2 - 1)$ and $(1/\lambda^2)$ for pure PVA and ZnO/ PVA nanocomposite films.
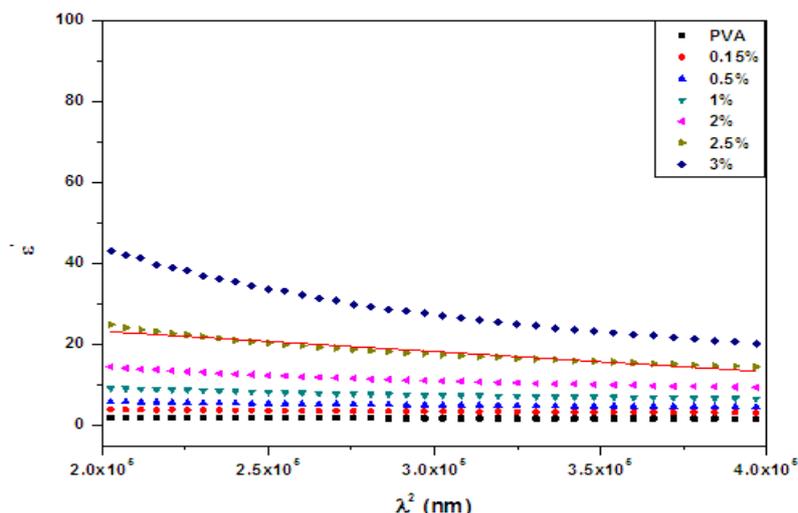
Fig. (8): Relation between ε' and λ^2 for pure PVA and ZnO/ PVA nanocomposite films.
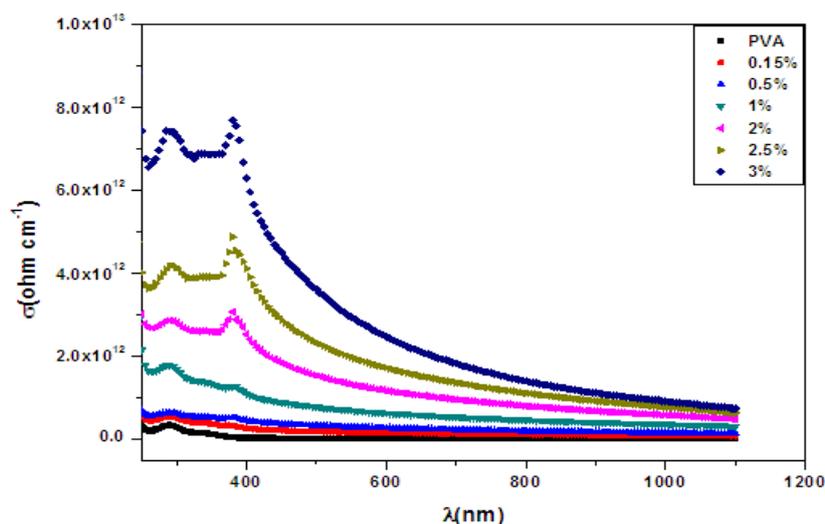
Fig. (9): The optical conductivity of pure PVA and ZnO/ PVA nanocomposite films.

Table (1): Dispersion parameters of ZnO/ PVA nanocomposite films at different concentration of ZnO.

ZnO%	E_g (eV)	E_o(eV)	E_d (eV)	E_o/ E_g	n_o	ε_1
0 %	3.82	5.1	3.86	1.34	1.33	1.77
0.15 %	3.56	4.54	8.47	1.28	1.69	2.86
0.5 %	3.33	4.39	13.38	1.32	2.01	4.04
1 %	3.31	4.23	19.72	1.28	2.38	5.66
2 %	2.86	3.93	25.67	1.37	2.75	7.56
2.5 %	2.83	3.73	38.26	1.32	3.36	11.29
3 %	2.78	3.67	54.54	1.32	3.98	15.84
average				1.32		

Table (2): The average oscillator strength S_o, and averages interband oscillator wavelength λ_o, free carriers (N/m^*), long wavelength refractive index n_∞, and long wavelength dielectric constant ε_∞ of the ZnO/ PVA nanocomposites.

Conc.	S_o $(m^{-2})*10^{13}$	λ_o (nm)	N/m^* $(m^{-3})*10^{21}$	ε_∞	n_∞
0 %	1.35	243.13	0.13	2.4	1.55
0.15 %	2.10	290.89	0.46	5.01	2.24
0.5 %	3.26	294.78	0.75	7.48	2.73
1 %	4.54	310.59	1.53	12.52	3.54
2 %	5.44	335.02	3.15	21.22	4.61
2.5 %	7.53	352.43	6.52	38.73	6.22
3%	8.56	380.81	14.2	73.07	8.55